

On the Impact of Adjacent Channel Interference in Multi-Channel VANETs

Claudia Campolo*, Christoph Sommer[†], Falko Dressler[†] and Antonella Molinaro*

*Università Mediterranea di Reggio Calabria, Italy. E-mail: name.surname@unirc.it

[†]University of Paderborn, Germany. E-mail: {sommer,dressler}@ccs-labs.org

Abstract—The efficient usage of multiple channels allocated for vehicular communications is deemed crucial to support the increasing spectrum demand of current and upcoming Intelligent Transportation Systems (ITS). In this context, an accurate modeling of adjacent channel interference (ACI) is needed to better understand its adverse effects on simultaneous communications on different channels. In this paper, we modeled ACI in the simulation framework Veins by strictly following the standard specifications in what concerns spectral emission masks. The model was validated in a set of experiments using off-the-shelf chipsets and a software defined radio. We then studied ACI effects at the physical and packet levels in multi-channel vehicular networks through extensive simulations. Our results clearly indicate that slightly larger delays and significantly lower reliability can be experienced when ACI is modeled. Insights are also provided about the usability of the devised ACI simulation model in future studies.

Index Terms—VANETs, multi-channel, IEEE 802.11p, adjacent channel interference.

I. INTRODUCTION

The huge data traffic demands of Vehicular Ad hoc Networks (VANETs) cause the continuously growing demand for bandwidth. VANET services are getting more advanced to improve road safety and traffic efficiency, while targeting a more comfortable driving and traveling experience. To address such capacity requirements, it is crucial to ensure an optimal exploitation of available radio resources. Multiple channels have been allocated worldwide in the spectrum around 5 GHz for IEEE 802.11p communications [1].

The intuitive benefit of a multi-channel spectrum is that it allows multiple services to be simultaneously provided over different channels with consequent throughput improvements. However, the parallel usage of adjacent channels may hinder successful communications, due to *adjacent channel interference* (ACI) [2]. A target receiver can be disturbed by an interfering signal from an adjacent channel that increases the interference level and, eventually, cause errors in the received packet. Similarly, a potential transmitter could be forced to defer its own transmission, if due to an interfering signal the clear channel assessment (CCA) mechanism detects the channel as busy. Such phenomena may severely affect the performance of many vehicular applications (e.g., safety applications), which could be penalized by large latency values and poor reliability.

Plenty of work on multi-channel VANETs has been proposed to make the best of few available channels, e.g., by distributing data traffic and offloading congested channels

reserved for safety communications [3]. However, to the best of our knowledge, just a few papers have analyzed ACI issues and proposed relevant countermeasures, e.g., [4], [5]. Only a set of preliminary experimental results has been provided [6]. Moreover, the support of ACI modeling in VANETs simulators is still missing, calling into question the accuracy of existing multi-channel studies.

In order to fill this gap, we investigate in details both *microscopic* effects (e.g., the received interference values) and *macroscopic* consequences of ACI at the transmitter and receiver side (i.e., increase of channel access delay and packet loss) over multi-channel communications. To this aim, we first perform a set of experiments with standard IEEE 802.11p devices as well as a software defined radio implementation [7] to get insights about the ACI emission and sensitivity in the real world. Then, we extended Veins [8], a well-known and widely used Open Source¹ vehicular network simulation framework built on top of the OMNeT++ network simulator. The latter one provides the support for the flexible and accurate modeling of signals over multiple frequencies, hence fulfilling the ACI modeling demands. We developed the ACI model by accounting for the latest standard specifications [9] and also carefully validated the model using results from the conducted experimentation. In this paper, we report on the ACI model and the validation but mainly focus on an extensive simulation study revealing many critical properties of ACI at a large-scale. In particular, we assess the impact of ACI on communication reliability and delay for critical distances between sender and receiver and under different load/co-channel interference settings.

The remainder of the paper is organized as follows. Section II discusses ACI in multi-channel VANETs, also providing details about performed experiments. Details about the modifications applied to Veins are provided in Section III. Simulation results are reported in Section IV. Section V elaborates on achieved findings to suggest future research directions that could take advantage of the conducted study. Finally, Section VI concludes the paper.

II. BACKGROUND AND MOTIVATIONS

A. Multi-channel VANETs

A bandwidth has been allocated in the 5 GHz spectrum worldwide for vehicular communications: 75 MHz in the

¹<http://veins.car2x.org/>

United States and 50 MHz in Europe. So far, one channel is reserved for the exchange of cooperative safety data traffic. Other channels may be used by other less critical applications and to offload the safety channel under congestion conditions [1].

As more complex Intelligent Transportation Services (ITS) use cases are going to be deployed in addition to basic safety and traffic efficiency warnings, spectrum demands get stronger. For instance, a dedicated channel is expected to be allocated for newly emerging services, e.g., platooning and autonomous driving [1]. In such a context, the design of efficient and effective channel selection policies gets more relevant. Static application-assigned channels and stove-pipe approaches filling the channels in specific order appear as the most straightforward options so far, although smarter and more flexible approaches, e.g., accounting for the actual channel load conditions, have to be pushed.

Any channel selection policy has to consider ACI phenomena caused by spurious emissions from nearby channels due to non ideal power masks, as detailed in the following.

B. ACI in 802.11p

The starting point to understand ACI effects and account for them is to analyze the spectral masks associated to communication devices as foreseen by standard regulations. They limit the out-of-band energy of a transmitter. More in detail, the mask specifies a frequency-dependent upper bound on the permitted power spectral density (PSD) of the transmitted signal. The spectral mask losses at a frequency offset of ± 10 MHz from the center frequency, corresponding to the adjacent channel carriers, are not negligible (see Table I) [9].

ACI may have adverse consequences on both the reception and the transmission dynamics. Specifically, a spurious signal increasing the interference level on a given channel could (i) increase the packet error rate (PER) at a receiver, and/or (ii) increase the channel access delay, i.e., the time a node spends in backoff before transmitting a packet, at a transmitter.

As concerns the first effect, PER occurs if the measured signal-to-interference-plus-noise ratio (SINR) at a receiver node is lower than the SINR threshold for the data rate at which the packet has been transmitted. This is the case of node B in the top of Figure 1, that cannot correctly receive a packet transmitted by node A due to the interference from node C transmitting over the adjacent channel. The ACI effects on the reception dynamics depend on the transmission power of the target transmitting and interfering nodes, the reciprocal distance between transmitter, receiver and interferer and the propagation environment as shown by Rai et al. [6] in the measured PER results.

If a node attempting to transmit a packet gets a channel busy indication from the CCA mechanism, due to an interfering signal from a transmitter tuned into an adjacent channel, it freezes its backoff counter and defers its own transmission, thus increasing the access delay. This is the case of node B in the bottom of Figure 1. Such a deferral may lead to wrongly prevent the packet transmission, even if the intended receiver (node A) could successfully decode the packet because it is

TABLE I
TRANSMITTER SPECTRAL MASK ACCORDING TO
[9, TABLE D-5, CLASS C]

Offset	Level
At the center frequency	0 dB
± 4.5 MHz	0 dB
± 5 MHz	-26 dB
± 5.5 MHz	-32 dB
± 10 MHz	-40 dB
± 15 MHz	-50 dB

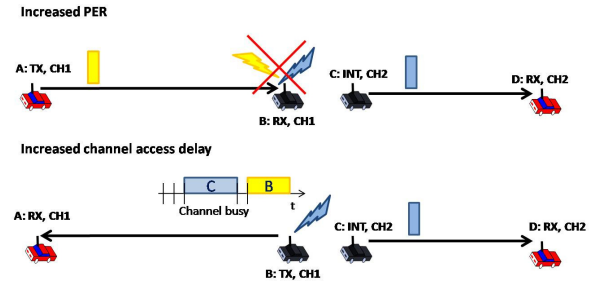


Fig. 1. ACI effects on reception (top) and transmission (bottom) dynamics.

not affected by the interferer (node C). More in detail, packet deferral occurs if the received power of the signal transmitted into the adjacent channel is higher than the carrier sense threshold (CST) condition which lets the CCA mechanism detect the channel busy. Such a packet deferral occurs at the transmitter side, regardless of the position of its intended receiver.

Campolo et al. [5] provide preliminary findings about ACI effects on transmission dynamics through an analytical model characterizing the access delay performance of unicast packets, under saturation conditions.

In this paper, we take a step forward to get further insights through a simulation study in Veins that we extended to support ACI. The study has been conducted under typical vehicular traffic pattern settings and accounting for the latest standard specifications for what concerns PSD values. Moreover, the impact of ACI on both transmission and reception dynamics has been derived, by also considering mixed co-channel and adjacent channel interference scenarios.

C. Experimental Validation

Before we set out to investigate the impact of ACI in computer simulations, we perform an experimental study to confirm the discussed effects in the real world – both in terms of ACI emission and susceptibility.

First, we examine the levels of ACI emitted by two representative devices. As our first device we use an embedded system running Linux 3.9, outfitted with a commercial off-the-shelf device: a UNEX DCMA-86P2 miniPCI card. This card has been used in measurements of IEEE 802.11p by researchers worldwide, notably many participants of the 2011 Grand Cooperative Driving Challenge (GCDC) [10], [11]. As our second device (to confirm that this effect is not just limited to off-the-shelf devices, but also present in specialized

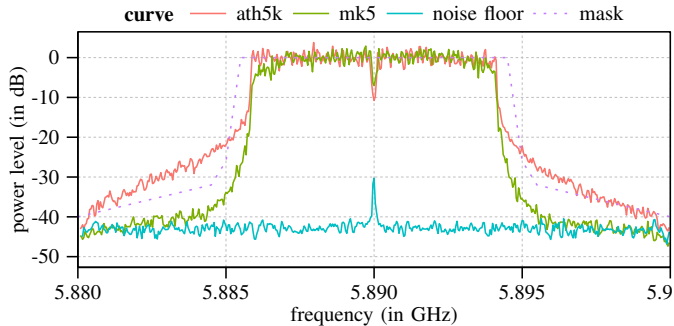


Fig. 2. Spectral mask of Table I (dotted) and qualitative spectrum measurements (solid) of 5.890 GHz transmissions with a nominal bandwidth of 10 MHz. Shown are measurements for transmissions of a UNEX DCMA-86P2 card with an Atheros AR5414A-B2B chip (top) and a Cohda MK5 device (middle) versus noise only (bottom).

equipment designed for field trials) we use a Cohda Wireless MK5, the company’s newest model of integrated vehicular networking systems. Cohda Wireless devices have been used for major field trials like the simTD project in Germany and the U.S. Safety Pilot initiative [12].

Figure 2 illustrates the results of our first experiment. To confirm our assumption about real world devices transmitting at not much narrower bandwidth than is mandated by the transmit spectral mask of Table I, we record frame transmissions by each device with an Ettus USRP B210 SDR. The figure shows power measurements of each device in an FFT plot, that is, a plot of power vs. frequency. Note that we do not report absolute measurements (dBm), but we report all measurements relative to the average maximum power recorded, so that the results are independent from effects like cable loss or antenna gain. We also include a plot of the noise floor, representative of the minimum average power that could be recorded. The figure is overlaid with the spectral mask of Table I to illustrate how the devices, indeed, roughly conform to its restrictions (the MK5 more so than the UNEX card). This confirms that, indeed, the spectral mask of Table I is a good approximation of emitted ACI.

To further confirm the sensitivity of real world devices to received ACI, we configure a second experiment. This experiment targets the increase of channel access delay caused by ACI triggering the CCA mechanism and deferring the transmission, as explained in the previous section. To get insights into the CCA mechanism’s operation in a real device, we employ the aforementioned Linux system containing a UNEX card, configure an independent virtual interface to monitoring mode, and record Radiotap² headers of sent frames. We use a modified version of the Linux kernel which amends all Radiotap headers with how long each frame was delayed in a transmit queue – from entering into the queue to being deleted. Thus, a longer delay of a frame would indicate that the transmit queue was blocked by CCA.

We set up one such system to continuously transmit frames on one channel. Another system located at the same premise at a short distance from the previous one was set up similarly, but

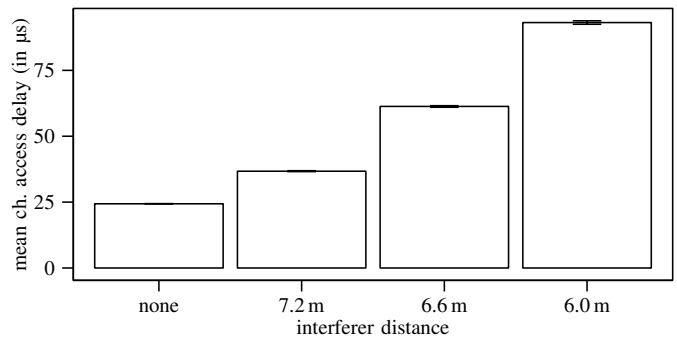


Fig. 3. Baseline measurements for channel access delay with no ACI (“none”) and increase in channel access delay brought about by the operation of an identical NIC on an adjacent channel, placed at different distances away from the target sender. Shown are measurement results for two UNEX DCMA-86P2 NICs.

on an adjacent channel. Note that, because of delays incurred in the software, by CSMA, and by post-transmit backoffs, neither device could saturate the channel on its own. Moreover, the transmit power was low enough to not reliably block channel access by the first device at larger distances. Still, due to random effects introduced by noise there is a certain probability of blocking the sender – and the probability should increase with the power level of interference (that is, with decreasing distance).

Figure 3 illustrates the results of this experiment, reporting queuing delays for measurements with the second device turned off, then set up at decreasing distance (7.2, 6.6 and 6.0 m). The impact of ACI on the channel access delay of a real device is clearly visible in the figure: the closer the interferer is set up, the more likely it is to delay transmissions, confirming the susceptibility of real world devices to received ACI and motivating us to deeply explore the phenomena.

III. EXTENDING VEINS TO SIMULATE ACI

Among available simulation platforms for performance evaluation of vehicular networks [13], we use Veins to evaluate the impact of ACI. This is because it offers an integrated traffic and network simulation framework, by extending the OMNeT++ network simulator [14], together with a realistic road traffic simulator SUMO [15]. Each Veins node at the physical (PHY) and medium access control (MAC) layers is implemented as a single-radio device with an IEEE 802.11p wireless network interface. Higher layers can be customized in terms of data traffic patterns (e.g., packet size, packet generation rate) according to the application to be simulated, e.g., safety/non-safety. Moreover, Veins inherits from OMNeT++ the support for the flexible and accurate modeling of signals over multiple frequencies, hence fulfilling the ACI modeling demands, as detailed in the following.

A. Devised additions

Veins relies on the MiXiM package [16] to simulate wireless and mobile networks. It models the wireless medium in all three dimensions (time, space and frequency). To represent a physical signal sent over the channel MAPPING instances

²<http://www.radiotap.org/>

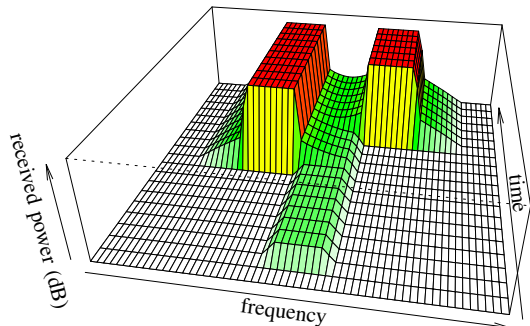


Fig. 4. Illustration of the ACI effect modeled in Veins using a three dimensional mapping (frequency, time, power): received signal strengths for three IEEE 802.11p devices strictly conforming to the spectral mask of Table I. Each device starts to transmit at a different time, operating at distances of 300 m (center frequency) and 3 m (adjacent channels) from the receiver.

are used for transmission power, bit-rate, attenuations and receiving power. They all represent mathematical mappings defining the according data over time and maybe more dimensions like frequency or space. In the current 802.11p Veins implementation, the attenuation over time is identical for every frequency within the signal bandwidth (10 MHz) and no signals are detected outside of such a bandwidth.

To account for the spectral mask losses as specified in standard documents, we leverage the utility methods provided by the MAPPINGUTILS class in MiXiM, that is highly flexible in modeling signals on multiple frequencies. Hence, we account for the fact that the real signal extends over a bandwidth larger than 10 MHz and its attenuation may change in the frequency domain. No changes occur in the time domain.

The CREATEMAPPING() function with a LINEAR interpolation is used to model the spectral mask of the received signal. In particular, such a method is invoked in the CREATESINGLE-FREQUENCYMAPPING() function of the BASEMACLAYER class where the transmission power mapping is set according to parameters passed by the MAC layer class (i.e., the start and end time of the frame, the central frequency, the channel bandwidth and the transmission power).

No attenuation is assumed within the ± 4.5 MHz bandwidth. The transmission power is decreased by the attenuation values specified for the frequency offsets in Table I; the resulting frequency, time, power mapping is illustrated in Figure 4.

Hence, once the mask of a received signal from an adjacent channel is derived by a node, channel-induced attenuation (e.g., due to path loss, obstacles, etc.) is computed and the signal is classified either as below the reception sensitivity threshold or strong enough to contribute to the detected interference. More in detail, according to the status of the node (i.e., receiving, transmitting) the detected signal from the adjacent channel may either hurt packet reception, being accounted for by the SINR, or triggers a busy channel indication.

Modifications have been applied to Veins version 4 alpha 2. PHY and MAC routines are not affected at all.

IV. PERFORMANCE EVALUATION

We leverage the extended Veins simulator to assess to which extent ACI could affect both transmission and reception

dynamics. Since our goal is to gain initial, but fundamental insights we decided to consider simplistic scenarios, both in terms of mobility and propagation, in order to ease the interpretation of results. Microscopic ACI effects are captured by measuring physical layer parameters, i.e., the interfering received power from a single and multiple nodes transmitting on an adjacent channel. Macroscopic ACI effects are then evaluated by measuring packet-level metrics that affect reliability and latency performance.

A. Microscopic ACI effects

As a first step we derive the interfering received power under different transmission power and transmitter-interferer distance settings. In so doing, we can identify under which conditions ACI could affect channel busy detection mechanisms.

Figure 5 reports the measured received power at a target node due to an interfering signal from a transmitter tuned into an adjacent channel. Received power values account for attenuations due to Two-Ray Ground and spectral mask losses in Table I.

Due to an interferer on the adjacent channel using a 20 dBm transmission power, a potential transmitter gets a channel busy indication (received power higher than the CST set to -85 dBm) if the interferer is closer than 7 m.

For lower transmission power values, instead, ACI effects are almost negligible unless the interferer is very close (e.g., 1–2 m), which is a less realistic condition. However, the depicted distance bounds refer to the conditions of a *single interferer*.

Things get worse in the case of *multiple interferers*. Their transmission may cause a busy channel detection signal even if they are located farther from the intentional transmitter. To this aim we measure the received interference power sum in Figure 6 when varying the number of interferers (from 1 to 8) for a target node. The latter one and the interfering nodes positioned in the square scenario depicted in Figure 7(a), in the outer 10 m-, 20 m-, 30 m-large square ($d=5$ m, $d=10$ m, $d=15$ m respectively), are tuned into adjacent channels. It is worth noticing that thanks to CSMA, it is quite unlikely that several nodes transmit at the same time. However, it could be a reasonable assumption if such interferers are not under each other's coverage, e.g., vehicles approaching an intersection from different roads, and/or tuned into different channels adjacent to the target node's channel. The transmission power of interfering nodes, P_t , is set to 20 dBm. If the distance is 5 m, one interferer is enough to let the target node declare the channel busy, at 10 m and at 15 m at least two and six interferers are required, respectively.

B. Macroscopic ACI effects

Next steps are aimed to explore the ACI effects on the packet transmission and reception dynamics, by understanding to which extent the measured interference power values result in increased access delay and losses values.

Two different topologies are considered. The first scenario is the square depicted in Figure 7(a). Metrics are derived for the node in the middle (the shaded vehicle) when varying the number of interferers (red vehicles) and the side length

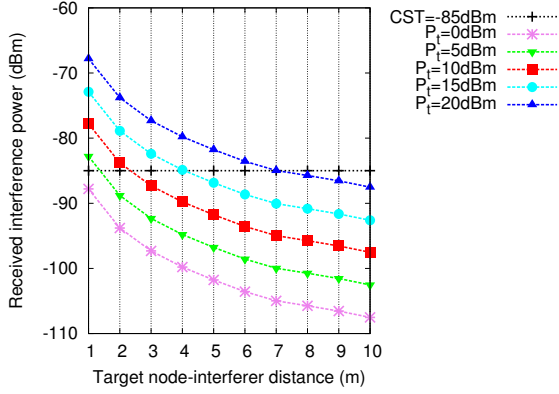


Fig. 5. Received interfering power at a target node from an interferer located at a varying distance for different transmission power settings.

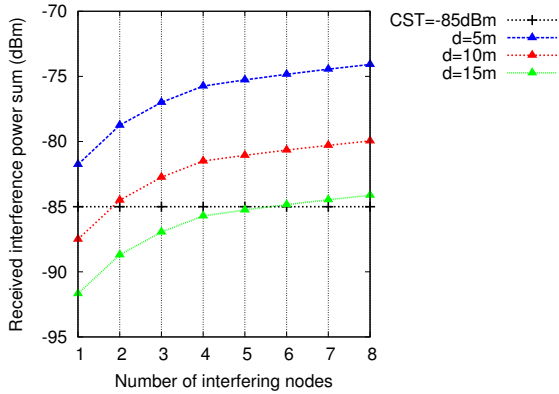
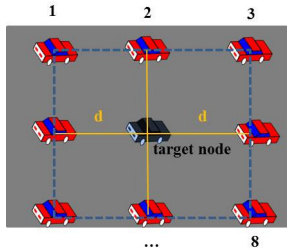
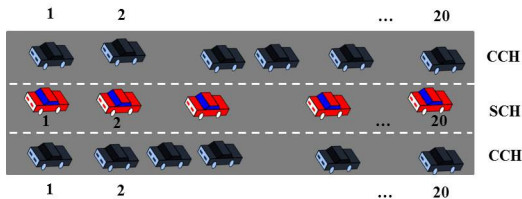


Fig. 6. Interference power sum at a target node vs. the number of interfering nodes tuned into the adjacent channel when varying interferer-target node distance ($P_t=20$ dBm).



(a) Square scenario: the shaded vehicle is the target node and nearby red vehicles in the square (with side= $2d$) are interfering nodes.



(b) Highway scenario: vehicles (5, 20) in the middle lane are tuned into the SCH, vehicles in the leftmost and rightmost lanes (20+20) are tuned into the CCH.

Fig. 7. Simulation scenarios.

d (5 and 10 m). The second scenario resembles a three-lanes highway, Figure 7(b), with up to 60 vehicles. Inter-vehicle distance per each lane follows an exponential distribution, proved to be a good fit for highway vehicle traffic [17], with mean equal to 50 m [18]. Forty vehicles in the external lanes transmit on the same channel, while vehicles in the middle lane transmit on an adjacent channel. For the sake of clarity, and without loss of generality, in the following we refer to *SCH* for the middle lane and *CCH* for the other two lanes.

In both scenarios, all nodes transmit their packets in broadcast, according to the traffic pattern summarized in Table II, along with PHY and MAC parameters, closely following the standard specifications [9].

Transmission dynamics. Results in Figure 8 show the average packet access delay at the target node. The number of active interferers, transmitting over the adjacent channel, in the 10 m large square is varied. The spectral mask in Table I has been considered to model ACI. We set the packet inter-arrival (T) to 100 ms and we varied the packet size (P) to resemble: (i) common vehicular traffic patterns, e.g., cooperative beaconing applications ($P=300$ B) and (ii) heavier load conditions, e.g., platooning and cooperative autonomous driving ($P=1000$ B) [1]. As expected, the access delay increases with the number of interfering nodes due to the higher contention on the medium. Moreover, the delay increases with larger packets that occupy the channel for a longer time. Values get close to 5 ms, when all 8 interferers transmit.

We repeat the experiments in a larger ($d=10$ m) square when all 8 surrounding vehicles transmit their packets, either into the same channel of the target node (box labeled as *Same channel*) or in the adjacent channel (box labeled as *Adjacent channels*). Results are reported in Figure 9. In such a case, a single interfering signal on an adjacent channel is not enough to trigger the channel busy. However, it can be noticed that there are still some ACI effects on access delay³, due to cumulative interference from multiple nodes that may transmit simultaneously. ACI impact is almost halved compared to the previous case ($d=5$ m, 8 interferers), where interferers are closer to the target node. Moreover, the ACI effect is clearly less detrimental than the effect of co-channel interference: shorter delay values are experienced.

When moving to the highway scenario, we keep $P=1000$ B. Figure 10(a) reports the access delay of vehicles tuned on the CCH and SCH, when ACI is modeled in the simulator with spectral masks in Table I (box labeled as *wACI*) and when ideal spectral masks are considered, as commonly assumed in existing multi-channel simulation studies (box labeled as *woACI*), when 5 and 20 vehicles are deployed in the middle lane. As expected, under the considered settings, the effect of co-channel interference on contention is more detrimental than the one due to ACI, whatever the channel vehicles are tuned into. Delay values very slightly increase for vehicles tuned into the CCH when ACI effects are simulated. This is because the interference generated by 40 vehicles transmitting on the same channel is heavier than the one due to 5-20 vehicles on the

³In absence of ACI, since a single transmitter is considered, only CSMA parameters contribute to the channel access delay values.

TABLE II
MAIN SIMULATION PARAMETERS

Parameter	Value
Transmission data rate R	6 Mbit/s
Packet inter-arrival T	100 ms
Packet size P	300–1000 B
Communication mode	Broadcast
Carrier Sense Threshold (CST)	-85 dBm
Transmission power	20 dBm
Access category	AC_VI
Number of runs	10
Simulation duration	60 s

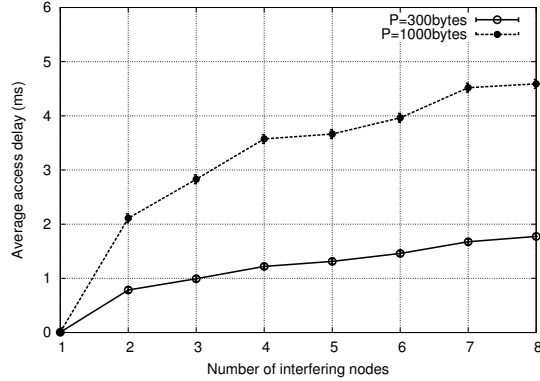


Fig. 8. Average access delay for the target node vs. the number of interfering nodes tuned into the adjacent channel ($d=5\text{m}$).

adjacent channel. The delay for vehicles on SCH significantly increases when the number of nodes on the SCH passes from 5 to 20. The impact of ACI, instead, leads to negligible increase of the delay values, with slightly higher increase for nodes on the SCH (40 vehicles on the CCH may potentially interfere with their transmission).

Reception dynamics. In order to have an understanding of how reception is affected by ACI, we derive the increase of the number of lost packets due to ACI in the highway scenario⁴. The metrics is computed as the percentage of additional packets that are not successfully received due to ACI effects w.r.t. the losses measured when ACI is not modeled. Results are reported in Figure 10(b). Losses over the CCH increase by around 16% when the number of nodes transmitting over the SCH is 5. Such value gets equal to around 45% when 20 nodes transmit over the SCH. Loss performance over the SCH is more affected by ACI than over the CCH. Indeed, the number of interferers over the CCH located in the nearby lanes is larger than the number of interferers tuned into the same channel, hence there is a higher probability that reception of packets gets corrupted.

V. FINAL REMARKS AND FUTURE RESEARCH DIRECTIONS

Despite being preliminary, the study provided the following main interesting findings:

- The effect of ACI into the channel access behaviour has not to be neglected for common transmission power

⁴Contrarily to the small square scenario, it allows to average results over a large set of receivers, as it would be for broadcast transmissions in VANETs.

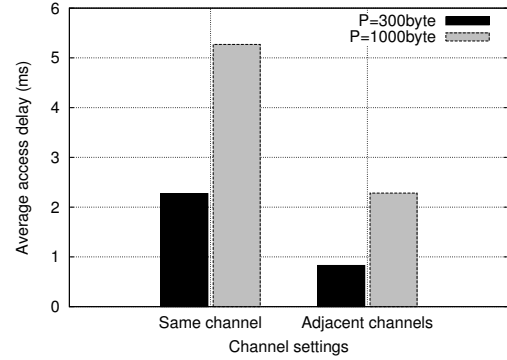
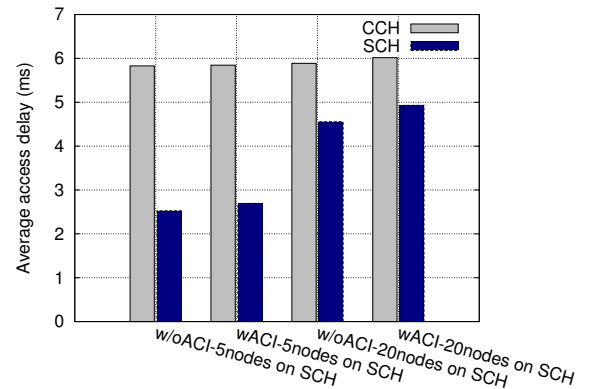
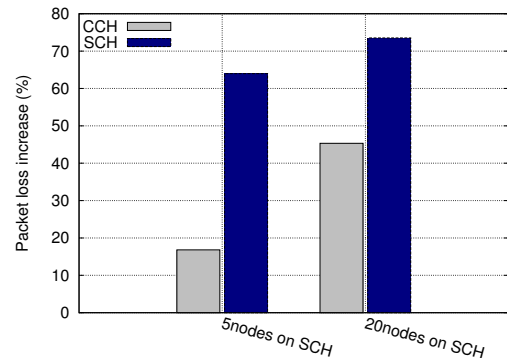


Fig. 9. Average access delay for the target node in presence of 8 interfering nodes tuned into the same channel (*Same channel*) and into the adjacent channel (*Adjacent channels*) ($d=10\text{m}$).



(a) Average access delay with and without ACI effects



(b) Packet loss increase due to ACI

Fig. 10. Metrics computed in the highway scenario with 40 vehicles over the CCH and a varying number of nodes over the SCH.

settings (e.g., 20 dBm), when the involved nodes are at a distance lower than 7 m. Such settings could characterize, for instance, vehicles on adjacent lanes, in a platoon, parked in parking lots, or in a traffic jam.

- Under the aforementioned distance settings, ACI impact may be negligible when considering transmission power values lower than 20 dBm. This would, for instance, suggest the possibility to use adjacent channels in different (nearby) platoons to reduce interference and preserve communications requirements (e.g., low latency and high reliability).

- The increase of channel access delay due to ACI is largely negligible when co-channel interference is also experienced.
- Results mainly show that the increased number of losses is the more evident effect of ACI in mixed co-channel and ACI scenarios. Losses due to ACI cannot be overlooked. They are especially detrimental since the majority of packets in VANETs is expected to be delivered in broadcast and, hence, losses cannot be recovered.

This paper is only the first step towards a set of future works, which could benefit from the achieved findings and provide further insights, described as follows.

ACI effects under different and more realistic settings.

The effects of ACI when coupled with other channel/topology-induced phenomena (e.g., obstacles) and other more loaded traffic conditions should be assessed. Moreover, the impact of different access category parameters used over adjacent channels would be worth to be investigated. Being transmission power adaptation among the main solutions to counteract channel congestion [1], for the sake of completeness, the impact of ACI should be analyzed under different transmission power settings for different nodes over different channels. To improve the accuracy of the ACI modeling, the receiver adjacent channel rejection values, as reported in the standard specifications [9], should be considered. Further experimental results could be valuable to evaluate how commercial devices meet such rejection values and give input to simulators.

ACI in channel selection. The devised accurate simulation modeling of ACI phenomena would facilitate the design and evaluation of smart channel selection schemes in multi-channel VANETs, aimed to improve spectrum usage, while meeting data delivery requirements. For instance, the channel selection policy could select the less interfered channel by accounting both for co-channel and adjacent channel interference in terms of channel busy ratio, directly measured or advertised by nearby nodes in a cooperative manner as for congestion control mechanisms [1]. The ACI modeling could allow to accurately assess the performance of proposed solutions, so to shed light into the actual available capacity of the allocated spectrum in sustaining different traffic demands.

ACI in multi-radio devices. To really exploit the available multiple channels and meet the increasing spectrum demand, vehicular devices are expected to be equipped with multi-radio transceivers, able to leverage multiple channels at a time. ACI among radio transceivers located on the same vehicle could be a serious issue that entails a careful evaluation of antenna configuration, near field propagation effects, cabling issues and wiring costs. Achieved findings would help the design of specific rules aimed to coordinate transmissions on the multiple radios at the MAC layer. At the PHY layer, self-interference cancellation techniques are getting mature in the context of full-duplex (FD) transceivers and could be applied for multi-radio transceivers. However, their prototyping is still at its infancy and far from being integrated in off-the-shelf chip solutions. The existing literature targeting FD communications mainly focuses on simultaneous transmission/reception over the same frequency. Although self-interference cancellation could mitigate ACI effects, it is still important to accurately

measure ACI since such measures can be used as an input to MAC protocols aiming to improve FD performance.

VI. CONCLUSIONS

The paper discusses ACI phenomena in VANETs and the need to accurately model them to improve the realism of simulations, given the growing interest in multi-channel solutions to support the wide range of vehicular applications. We describe how we modified Veins to simulate ACI, after experiments with real devices, and report some results to see its impact into packet transmission and reception dynamics in some simple, but representative, scenarios. Further studies on ACI are highly encouraged to improve the design of advanced PHY/MAC layer solutions for multi-channel VANETs.

REFERENCES

- [1] C. Campolo, A. Molinaro, and R. Scopigno, "From today's VANETs to tomorrow's planning and the bets for the day after," *Elsevier Vehicular Communications*, vol. 2, no. 3, pp. 158–171, 2015.
- [2] V. Angelakis, S. Papadakis, V. Siris, and A. Traganitis, "Adjacent Channel Interference in 802.11a Is Harmful: Testbed Validation of a Simple Quantification Model," *IEEE Communications Magazine*, vol. 49, no. 3, pp. 160–166, 2011.
- [3] F. Klingler, F. Dressler, J. Cao, and C. Sommer, "MCB - A Multi-Channel Beaconing Protocol," *Elsevier Ad Hoc Networks*, Aug. 2015, in print, available online: 10.1016/j.adhoc.2015.08.002.
- [4] R. Lasowski, F. Gschwandtner, C. Scheuermann, and M. Duchon, "A Multi Channel Synchronization Approach in Dual Radio Vehicular Ad-Hoc Networks," in *73rd IEEE VTC2011-Spring*, IEEE, May 2011.
- [5] C. Campolo, A. Molinaro, and A. Vinel, "Understanding Adjacent Channel Interference in Multi-channel VANETs," in *6th IEEE VNC 2014*, IEEE, Dec. 2014, pp. 101–104.
- [6] V. Rai, F. Bai, J. Kenney, and K. Laberteaux, "Cross-Channel Interference Test Results: A report from the VSC-A project," IEEE, Presentation 802.11 11-07-2133-00-000p, Jul. 2007.
- [7] B. Bloessl, M. Segata, C. Sommer, and F. Dressler, "Towards an Open Source IEEE 802.11p Stack: A Full SDR-based Transceiver in GNURadio," in *5th IEEE VNC 2013*, IEEE, Dec. 2013, pp. 143–149.
- [8] C. Sommer, R. German, and F. Dressler, "Bidirectionally Coupled Network and Road Traffic Simulation for Improved IVC Analysis," *IEEE Trans. on Mobile Computing*, vol. 10, no. 1, pp. 3–15, Jan. 2011.
- [9] "Wireless LAN Medium Access Control (MAC) and Physical Layer (PHY) Specifications," IEEE, Std 802.11-2012, 2012.
- [10] A. B. Reis, S. Sargento, F. Neves, and O. K. Tonguz, "Deploying Roadside Units in Sparse Vehicular Networks: What Really Works and What Does Not," *IEEE Trans. on Vehicular Technology*, vol. 63, no. 6, pp. 2794–2806, Jul. 2014.
- [11] A. Geiger, M. Lauer, F. Moosmann, B. Ranft, H. Rapp, C. Stiller, and J. Ziegler, "Team AnnieWAY's entry to the 2011 Grand Cooperative Driving challenge," *IEEE Trans. on Intelligent Transportation Systems*, vol. 13, no. 3, pp. 1008–1017, Apr. 2012.
- [12] H. Rakouth et al., "V2X Communication Technology: Field Experience and Comparative Analysis," in *FISITA World Automotive Congress*, Springer, Nov. 2012, pp. 113–129.
- [13] C. Sommer, J. Härrä, F. Hrizi, B. Schünemann, and F. Dressler, "Simulation Tools and Techniques for Vehicular Communications and Applications," in *Vehicular ad hoc Networks - Standards, Solutions, and Research*, Springer, 2015, pp. 365–392.
- [14] A. Varga, "The OMNeT++ Discrete Event Simulation System," in *European Simulation Multiconference (ESM 2001)*, Jun. 2001.
- [15] D. Krajzewicz, G. Hertkorn, C. Rössel, and P. Wagner, "SUMO (Simulation of Urban MObility): An Open-source Traffic Simulation," in *MESM 2002*, Sep. 2002, pp. 183–187.
- [16] K. Wessel, M. Swigulski, A. Köpke, and D. Willkomm, "MiXiM – The Physical Layer: An Architecture Overview," in *2nd ACM/ICST SIMUTools 2009*, ACM, Mar. 2009.
- [17] F. Bai and B. Krishnamachari, "Spatio-temporal variations of vehicle traffic in VANETs: facts and implications," in *6th ACM VANET 2009*, ACM, Sep. 2009, pp. 43–52.
- [18] M. Boban, T. Vinhosa, J. Barros, M. Ferreira, and O. K. Tonguz, "Impact of Vehicles as Obstacles in Vehicular Networks," *IEEE JSAC*, vol. 29, no. 1, pp. 15–28, Jan. 2011.